



## OPEN ACCESS

## EDITED BY

Shihai Deng,  
Xi'an Jiaotong University, China

## REVIEWED BY

Zhifeng Hu,  
Beijing Academy of Science and  
Technology, China  
Xiaowei Wang,  
Beijing Technology and Business  
University, China  
Qiang Kong,  
Shandong Normal University, China

## \*CORRESPONDENCE

Qi Zhang,  
✉ qzhang@ecjtu.edu.cn  
Zheng Liang,  
✉ twyliang@126.com

## SPECIALTY SECTION

This article was submitted to Water and  
Wastewater Management,  
a section of the journal  
Frontiers in Environmental Science

RECEIVED 31 October 2022

ACCEPTED 12 December 2022

PUBLISHED 22 December 2022

## CITATION

Zhang Q, Liang Z, Guan X, Liang J and  
Gao P (2022), Application of  
iron-carbon microbial galvanic  
activated sludge combined with MBR  
process in the treatment of wastewater  
from comprehensive railway station.  
*Front. Environ. Sci.* 10:1085386.  
doi: 10.3389/fenvs.2022.1085386

## COPYRIGHT

© 2022 Zhang, Liang, Guan, Liang and  
Gao. This is an open-access article  
distributed under the terms of the  
[Creative Commons Attribution License  
\(CC BY\)](https://creativecommons.org/licenses/by/4.0/). The use, distribution or  
reproduction in other forums is  
permitted, provided the original  
author(s) and the copyright owner(s) are  
credited and that the original  
publication in this journal is cited, in  
accordance with accepted academic  
practice. No use, distribution or  
reproduction is permitted which does  
not comply with these terms.

# Application of iron-carbon microbial galvanic activated sludge combined with MBR process in the treatment of wastewater from comprehensive railway station

Qi Zhang<sup>1\*</sup>, Zheng Liang<sup>2\*</sup>, Xiaotao Guan<sup>1</sup>, Jingwen Liang<sup>1</sup> and Pan Gao<sup>1</sup>

<sup>1</sup>School of Civil Engineering and Architecture, East China Jiaotong University, Nanchang, China,

<sup>2</sup>Planning and Standard Research Institute, The National Railway Administration of the Republic of China, Beijing, China

The application of iron-carbon microbial cell activated sludge (ICMC-AS) was carried out in a membrane bioreactor (MBR) processor to treat wastewater from an integrated railway station. Results showed that the chemical oxygen demand (COD), total nitrogen (TN), and total phosphorus (TP) removal efficiencies of the original MBR processor increased from 80%, 30%, and 10% to 92%, 93.5%, and 92%, respectively. Further research showed that the combined sewage treatment system also had a strong impact resistance ability. The combined sewage treatment system ran stably when the COD, TN, and TP concentrations changed greatly. The in-depth analysis of the reaction process and reaction rate of the combined sewage treatment system revealed that the combined system is dominated by COD removal with high nitrogen removal efficiency. The removal rate constants of various pollutants were in the order:  $K_{\text{COD}}$  ( $0.647 \pm 0.017$ ) >  $K_{\text{NO}_3\text{-N}}$  ( $0.416 \pm 0.044$ ) >  $K_{\text{NH}_4\text{-N}}$  ( $0.275 \pm 0.014$ ) >  $K_{\text{TN}}$  ( $0.258 \pm 0.083$ ). Calculations of the energy saving and carbon emission reduction of the combined system showed that the system's annual carbon emission reduction could reach more than 388,203.55 kg CO<sub>2</sub>e, which remarkably improves the carbon emission reduction effect and obtains a good green effect. The results indicate that adding ICMC-AS to the MBR processor for combined wastewater treatment can substantially improve the efficiency of wastewater treatment and obtain better energy-saving and emission-reducing effects. This combined application provides an effective way for the transformation and upgrading of small- and medium-scale water treatment systems.

## KEYWORDS

railway wastewater, micro-electrolytic, iron-carbon microbial galvanic cell, combined wastewater treatment, MBR, carbon emissions

## 1 Introduction

The basic principle of wastewater treatment by activated sludge is based on a series of electrochemical and microbial reactions, such as microelectrolysis and electronic exchange (between different microorganisms, between microorganisms and various organic or inorganic substances, and between various substances) in the water formed by iron–carbon galvanic cells. A large number of studies have shown that microelectrolysis has a remarkable degradation effect on refractory substances in sewage treatment (Deng et al., 2020a). However, the application mechanism and removal efficiency of biochemical water treatment under the action of microelectrolysis are not clear because of the complexity of the microelectrolysis process. Current research on microelectrolysis wastewater treatment focuses on iron and carbon microelectric decontamination technologies. For example, Deng et al. developed a microelectrolytic process coupled with microbial nitrogen removal, which is a contact oxidation process based on the loading of microelectrolytic biological carrier formed by mixing  $\text{Fe}^0$  and activated carbon. The process removes nitrogen under micro-oxygen condition. The  $\text{NH}_4^+\text{-N}$  and TN removal efficiencies of this process were 92.6% and 95.3%, respectively (Deng et al., 2016a). Hu et al. developed an iron-rich substrate (IRS) based on iron–carbon microelectrolysis that can be used for sediment and overlying water remediation.  $\text{NH}_4^+\text{-N}$ ,  $\text{PO}_4^{3-}\text{-P}$ , organo-N, organo-P, TN, and total phosphorus (TP) in the overlying water were reduced by 48.6%, 97.9%, 34.2%, 67.1%, 53.2%, and 90.4%, respectively, by IRS during the 90 day long-term restoration. Moreover,  $\text{NO}_3^-\text{-N}$ ,  $\text{NH}_4^+\text{-N}$ , and organic N in sediments were reduced by 98.5%, 26.5%, and 6.3%, respectively (Hu et al., 2020).

Engineering applications are mostly carried out by iron and carbon microelectrolysis combined with biochemical decontamination technology. For example, Qi et al. applied microelectrolysis combined with sequencing batch reactor process to treat oxytetracycline production wastewater. When the influent chemical oxygen demand (COD) was 500 mg/L, the average COD removal rate increased from 76.1% to 94.4% (Qi et al., 2016). Microelectrolysis combined with expanded granular sludge bed and anaerobic/oxic system was used to treat oxytetracycline production wastewater. The oxytetracycline removal rate in the microelectrolysis reaction cell reached more than 95% (Wu et al., 2016).

In this study, iron–carbon microbial cell activated sludge (ICMC-AS) was formed by implanting iron–carbon-based materials into activated sludge microbial mass. ICMC-AS + membrane bioreactor (MBR) process was used for wastewater treatment in an integrated railway station. In order to solve the pollution problem of low nitrogen, phosphorus and other refractory elements in the original MBR reactor. The reaction principle of ICMC-AS is shown in Equations 1–4. The operation law of the combined processing system was obtained by studying its operation efficiency and parameters. The application mechanism of biochemical water treatment under the action of microelectrolysis was clarified through in-depth analysis of the

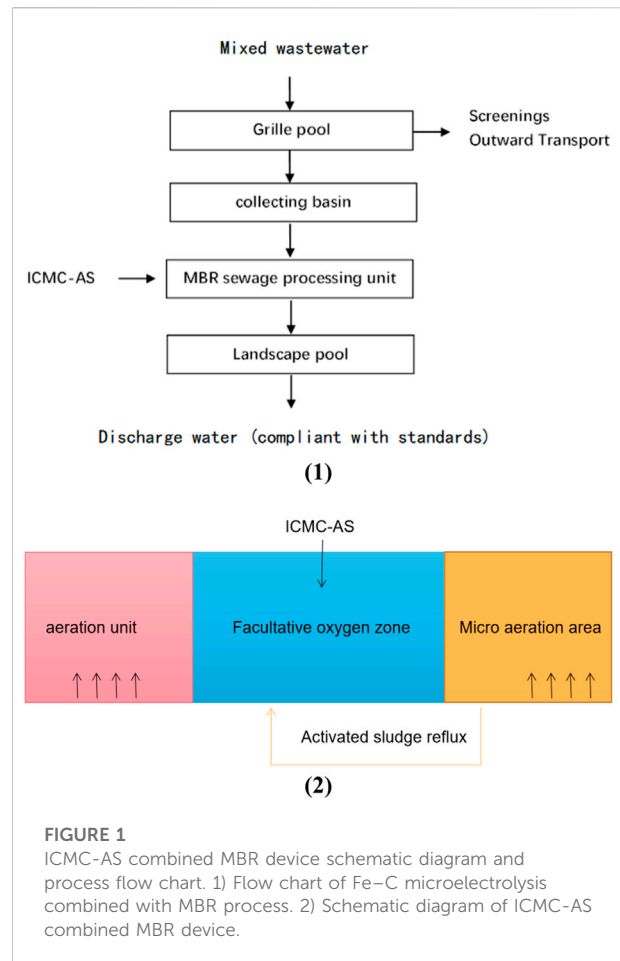
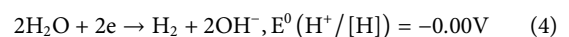
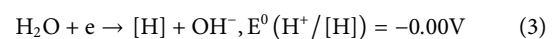
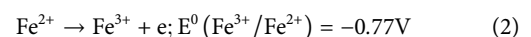
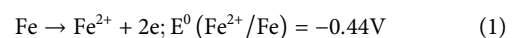


**FIGURE 1**  
ICMC-AS combined MBR device schematic diagram and process flow chart. 1) Flow chart of Fe–C microelectrolysis combined with MBR process. 2) Schematic diagram of ICMC-AS combined MBR device.

reaction process and mechanism of the iron–carbon-based microelectrolysis wastewater treatment system. This study provides an effective way for the transformation and upgrading of small- and medium-scale water treatment systems. It also provides technical support and research data basis for the application of microelectrolysis in sewage treatment technology.



## 2 Materials and methods

### 2.1 Sewage treatment equipment and raw sewage main quality

The main body of the sewage treatment equipment is an integrated MBR reactor. Raw sewage was used to discharge

wastewater from a comprehensive railway station, which consists of a railway passenger station, a large warehouse area, and related supporting facilities. The water quality indexes were COD levels of 100–400 mg/L,  $\text{NH}_4^+\text{-N}$  concentrations of 15–45 mg/L, TN concentrations of 20–60 mg/L, and TP concentrations of 2–6 mg/L.

## 2.2 Sewage treatment process

As shown in [Figure 1 1](#)) sewage from the integrated railway station was collected through the pipeline to the grid pool of the sewage treatment plant. Inorganic suspended matter in the sewage was removed through a thick and fine grid to reduce the wear on the subsequent pipelines and equipment. The effluent enters the catchment pool. As shown in [Figure 1 2](#)) A large number of facultative aerobic bacteria are contained in the facultative MBR system and can degrade organic matter in sewage by the dual action of microelectrolysis and facultative bacteria metabolism to degrade macromolecular organic pollutants into small molecular organic matter, which are eventually oxidized and decomposed into stable inorganic substances. Such as carbon dioxide and water. Moreover, power consumption is reduced, because the generation of facultative bacteria does not need the guarantee of dissolved oxygen (DO). The main function of aeration in a sewage treatment system is to scour and shock membrane filaments, and the DO produced can be used to oxidize a part of the small molecular organic matter and maintain the DO value of the effluent to ensure the normal microbial metabolism in the combined MBR system with concurrent oxygen microelectrolysis.

The design scale of the combined treatment system is 400 m<sup>3</sup>/day, the design total sludge age is infinite, the organic residual sludge discharge is nearly “zero” discharge, the mixed liquid concentration (MLSS) is 8000–20000 mg/L, and the sludge load is 0.02–0.10 kg COD/(kg MLSS-day).

## 2.3 Preparation of iron–carbon-based materials

The iron–carbon-based material consisted of 40%–50% elemental iron powder (300 mesh), 35%–42% activated carbon powder (200 mesh), 6%–8% metal catalyst (made of various metals), 5%–8% adhesive, and foaming agent, etc. The materials were mixed evenly to prepare 1–2 cm balls, which were dried at 105 C for about 2 h in a drying oven, preheated at 600 C for half an hour in a muffle furnace, and heated at 1000 C for 3 h. After annealing and cooling, the balls were crushed and sifted to retain particles below 150 mesh. The time between production and use should not be too long and should be suitable for real-time production before use to

ensure the activity of iron powder and avoid excessive oxidation.

## 2.4 Analysis of operation parameters

### 2.4.1 Water quality index detection and analysis methods

The wastewater treatment efficiency of the new technology was determined by detecting the water quality indexes ( $\text{COD}_{\text{Cr}}$ ,  $\text{NH}_4^+$ ,  $\text{NO}_3^-$ ,  $\text{NO}_2^{2-}$ , TP, and TN) in and out of the MBR reactor and comparing with the corresponding indexes of the original MBR reactor without ICMC-AS.  $\text{COD}_{\text{Cr}}$  was determined by potassium dichromate method,  $\text{NH}_4^+$  was determined by sodium chlorite spectrophotometry,  $\text{NO}_3^-$  was determined by phenol disulfonic acid spectrophotometry,  $\text{NO}_2^{2-}$  was determined by N-(1-naphthol)-ethylenediamine spectrophotometry, and TP was determined by potassium persulfate oxidation and ultraviolet spectrophotometry. TN is the sum of the values of  $\text{NH}_4^+$ ,  $\text{NO}_3^-$ , and  $\text{NO}_2^{2-}$ .

### 2.4.2 Reaction process data detection and reaction rate analysis

Carbon–nitrogen reaction rate was determined and the reaction characteristics of the combined process were defined by detecting the concentration changes of COD,  $\text{NH}_4^+\text{-N}$ ,  $\text{NO}_3^-\text{-N}$ , and  $\text{NO}_2^-\text{-N}$  during the operation of the MBR reactor (sampling every 30 min). The carbon–nitrogen reaction rate was calculated by the Origin software.

### 2.4.3 Estimation methods for energy saving and carbon emissions

Energy saving and carbon emission were estimated from three aspects: power consumption, water consumption, and drug consumption. Power consumption was converted according to the removal rate of the major pollutant (TN) and the increase rate. Water consumption only included the backwashing water. Other supporting water was relatively small, and water condition changed greatly; therefore, it was not measured. Carbon emissions were calculated on the basis of  $\text{CO}_2$ .

## 3 Result and discussion

### 3.1 Variation characteristics of carbon, nitrogen, and phosphorus in the combined sewage treatment system

The data shown in [Figure 2 1](#)) show that the COD of the influent municipal sewage varies at 112–328 mg/L without regularity, and a large change in COD value will have a load impact on the water treatment system ([Vleeschauwer et al., 2020](#)). Studies have shown that such a load impact will often

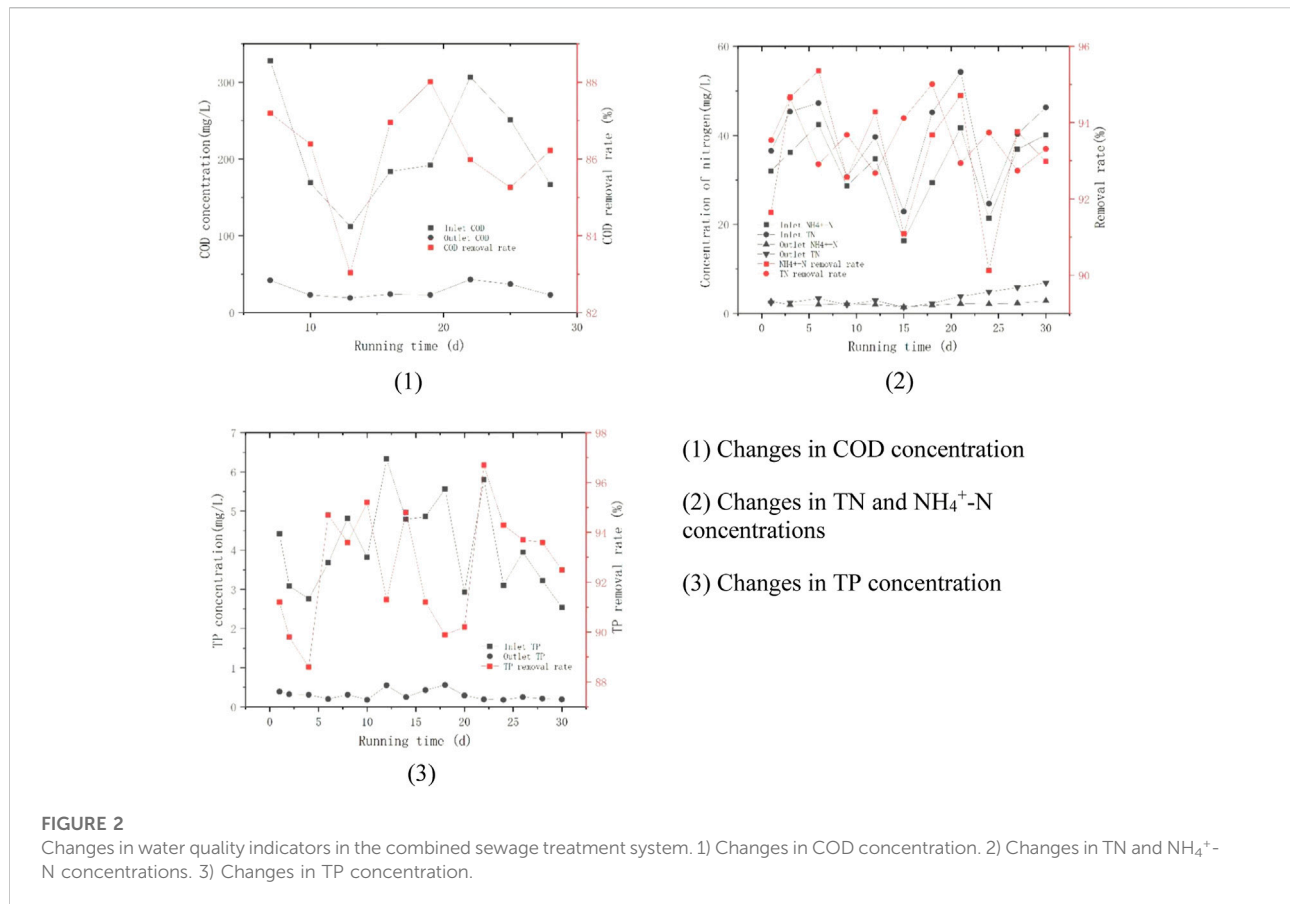


FIGURE 2

Changes in water quality indicators in the combined sewage treatment system. 1) Changes in COD concentration. 2) Changes in TN and NH<sub>4</sub><sup>+</sup>-N concentrations. 3) Changes in TP concentration.

have a great impact on the water treatment system (Yadu et al., 2019). Experimental data show that the sewage treatment system formed a larger organic shock load, the stable effluent COD value was between 19 and 43 mg/L, and the water COD and effluent COD values had a significant positive correlation. However, the ratio changed, which allowed the sewage treatment system to have a good performance and strong load impact resistance. Compared with the original MBR system without ICMC-AS, the COD removal rate of the combined system increased from 80% to 92%.

As shown in Figure 2 2), the NH<sub>4</sub><sup>+</sup>-N value measured at the inlet in the small test fluctuated greatly between 16 and 42 mg/L, and the TN value was between 2 and 55 mg/L, resulting in the large load impacts of NH<sub>4</sub><sup>+</sup>-N and TN on the sewage treatment system. The load impacts of NH<sub>4</sub><sup>+</sup>-N and TN loads have great influence on water treatment system (Meng et al., 2018). The NH<sub>4</sub><sup>+</sup>-N and TN values measured at the outlet were maintained at about 2–3 mg/L, indicating that the sewage treatment system has a strong ability to resist the load impacts of NH<sub>4</sub><sup>+</sup>-N and TN. In addition, the NH<sub>4</sub><sup>+</sup>-N and TN removal rates were about 93.5% and 94%, respectively, which are not much different from the removal rates in the laboratory. This finding indicates that the removal capacities for NH<sub>4</sub><sup>+</sup> and TN in the sewage treatment system were strong, and the current concentrations of NH<sub>4</sub><sup>+</sup> and TN did not

(1) Changes in COD concentration

(2) Changes in TN and NH<sub>4</sub><sup>+</sup>-N concentrations

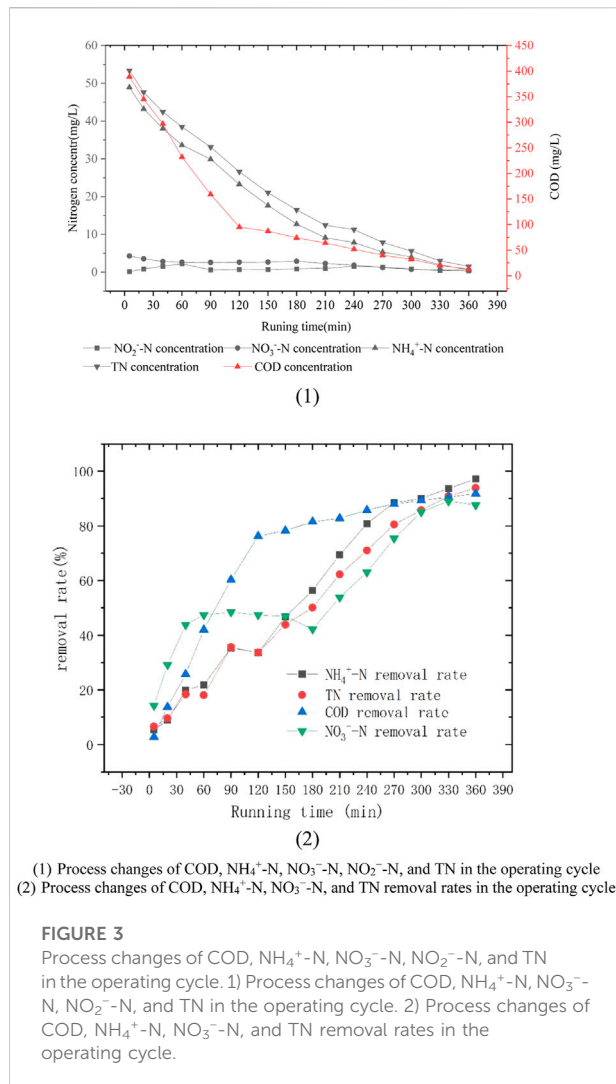
(3) Changes in TP concentration

reach the treatment limits. Additionally, the results show that the sewage treatment system has strong adaptability and adjustment ability and can maintain efficient nitrogen pollutant removal ability under a large load shock. Compared with the original MBR system without ICMC-AS, the NH<sub>4</sub><sup>+</sup>-N and TN removal rates increased from 40% and 30% to 93% and 93.5%, respectively, in the combined system.

As shown in Figure 2 3), the sewage treatment system has a good removal effect. TP values oscillated between 2 and 6 mg/L and were maintained at 0.3 mg/L after being treated by the sewage treatment system. This result indicates that the system had a stable treatment capacity for the TP of municipal sewage between 2 and 6 mg/L (most municipal sewage is within this range), and its removal rate was 92.58% on average. Compared with the original MBR system without ICMC-AS, the TP removal rate of the combined system increased from 10% to 92%.

### 3.2 Variation characteristics of carbon and nitrogen in the combined sewage treatment system during operation

As shown in Figure 3 1), COD was removed by rapid consumption within the first 120 min, and the value decreased

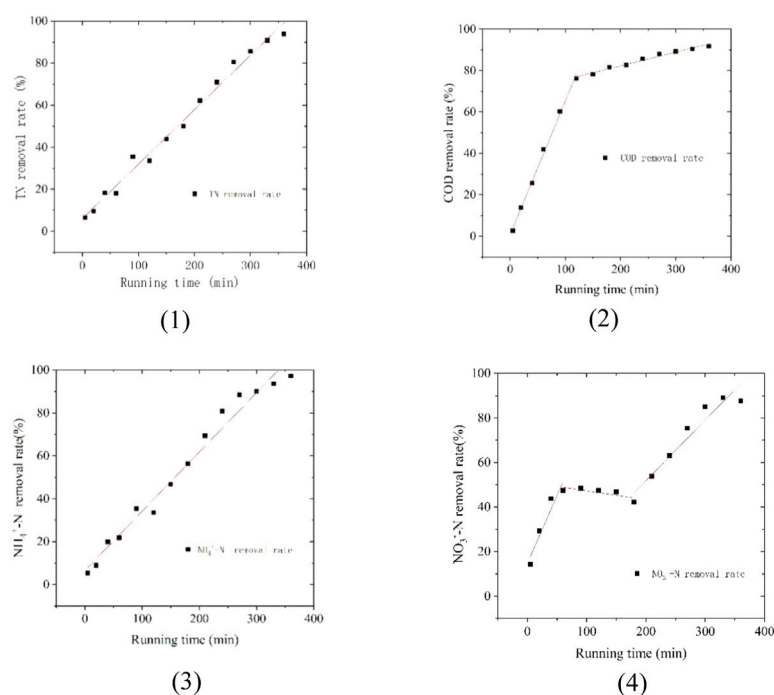


from 400 mg/L to 100 mg/L.  $\text{NH}_4^+$ -N decreased from 20 mg/L to 2.32 mg/L within 270 min, and  $\text{NH}_4^+$ -N decreased more slowly at 40–60 and 90–120 min. The DO values in these two periods oscillated between 0.2 and 0.3 mg/L, indicating that the biochemical reaction of the system was very violent between 0 and 120 min, which made the DO values hover between 0.2 and 0.3 mg/L and inhibited  $\text{NH}_4^+$ -N decomposition. However,  $\text{NO}_3^-$ -N concentration decreased from 5 mg/L to 2.81 mg/L between 0 and 40 min, increased from 2.58 mg/L to 2.89 mg/L between 40 and 180 min, and gradually decreased to 0.65 mg/L between 180 and 360 min. This finding is because the concentration change of  $\text{NO}_3^-$ -N is affected by nitrification and denitrification reactions, as well as the biochemical reactions of other elements (such as the biochemical absorption of iron and carbon) (Xing et al., 2016). Therefore, during the first 0–40 min,  $\text{NO}_3^-$ -N gradually entered the adsorption plane of various reactions and participated in various reactions. Therefore, its value was rapidly reduced to 2.81 mg/L. When these

participating reactions reached saturation or equilibrium state, it reflects the comparison between the rates of nitrification reaction ( $\text{NO}_3^-$ -N generation) and denitrification reaction ( $\text{NO}_3^-$ -N transformation and removal) (Deng et al., 2016b). When the rates of nitrification and denitrification reactions reach equilibrium, the value of  $\text{NO}_3^-$ -N will keep oscillating within a certain numerical range. However, when the denitrification reaction is larger than the nitrification reaction, the value of  $\text{NO}_3^-$ -N will gradually decrease. In this case,  $\text{NO}_2^-$ -N is usually seen as an intermediate product in the conversion of  $\text{NH}_4^+$ -N to  $\text{NO}_3^-$ -N (Deng et al., 2020b).  $\text{NO}_2^-$ -N accumulated gradually from 0 mg/L to 2.21 mg/L at 0–60 min, decreased to 0.61 mg/L at 40–90 min, accumulated gradually accumulated from 0.61 mg/L to 1.57 mg/L at 90–240 min, and then decreased to 0.35 mg/L at 240–360 min. In the whole process, the value of  $\text{NO}_2^-$ -N experienced two accumulation processes. More complex changes occurred. This change law does not accord with the characteristics of synchronous nitrification and denitrification or short-cut nitrification (Jiaohui et al., 2021; Wang et al., 2021; Tong et al., 2022a; Tong et al., 2022b). Therefore, based on the analysis of the change values of TN and DO, COD,  $\text{NH}_4^+$ -N,  $\text{NO}_3^-$ -N,  $\text{NO}_2^-$ -N, and DO are co-changing according to a certain correlation. DO showed periodic oscillations and repeated changes during the operation of the system. The changes in DO can be divided into three stages. In the first stage, the operation time of the treatment system was between 0 and 120 min, and the DO value in this period changed between 0.1 and 0.4 mg/L. In the second stage, the operation time of the treatment system was between 120 and 270 min, and the DO value in this period varied between 1.0 and 1.4 mg/L. In the third stage, the operation time of the treatment system was between 270 and 360 min, and the DO value in this period varied between 1.8 and 2.3 mg/L.

### 3.3 Carbon and nitrogen removal efficiency of the combined sewage treatment system

As shown in Figure 3 2), the change rate of the  $\text{NO}_3^-$ -N process value was close to that of COD at 40–60 min, indicating that the process of  $\text{NO}_3^-$ -N reaction during this period was equally dramatic. On the one hand, the reason is that many biochemical reactions of microorganisms in the system require the participation of  $\text{NO}_3^-$ -N. On the other hand, heterotrophic denitrification bacteria at this stage have sufficient organic carbon sources and a large amount of oxygen to efficiently carry out heterotrophic denitrification and consume  $\text{NO}_3^-$ -N. At 40–180 min, the  $\text{NO}_3^-$ -N process value hardly changed and was in a relative equilibrium state because of the lack of relative oxygen and the indominance of the number of relative denitrifiers in the whole system. However, from the analysis of TN removal rate, the overall TN removal rate was maintained at a relatively high growth level. Moreover, the change rates of the decomposition and process values of  $\text{NH}_4^+$ -N were also maintained



(1) TN rate fitting; (2) COD rate fitting; (3)  $\text{NH}_4^+\text{-N}$  rate fitting; (4)  $\text{NO}_3^-\text{-N}$  rate fitting

FIGURE 4

Carbon and nitrogen removal rates of the combined sewage treatment system. 1) TN rate fitting; 2) COD rate fitting; 3)  $\text{NH}_4^+\text{-N}$  rate fitting; 4)  $\text{NO}_3^-\text{-N}$  rate fitting.

at relatively high levels, which indicates that the nitrification and denitrification reactions were maintained at a relatively high dynamic balance. At 180–360 min, the change rate of the  $\text{NO}_3^-\text{-N}$  process value was relatively large, and the COD value dropped to 57 mg/L, which made the organic carbon source become relatively short, and the  $\text{NO}_3^-\text{-N}$  reaction process was transferred into the ICMC-AS. At this time, the organic carbon source materials (such as extracellular polymers, etc.) stored in ICMC-AS can be combined with the sufficient aerobic environment outside ICMC-AS to carry out heterotrophic denitrification, and the electron supply of ICMC-AS can be combined with the anoxic, facultative, and aerobic regions of MBR to carry out different degrees of autotrophic denitrification (Adav and Lee 2011; Pellicer-Nacher et al., 2013). Thus, an efficient denitrification reaction with a change rate similar to the process value of  $\text{NH}_4^+\text{-N}$  can be achieved.

### 3.4 Carbon and nitrogen removal rate of combined sewage treatment system

As shown in Figure 4, the reaction rate constants of each substance were obtained by fitting the COD,  $\text{NH}_4^+\text{-N}$ ,  $\text{NO}_3^-\text{-N}$ , and TN removal efficiencies. Among them, the  $K_{\text{COD}}$  (0–120 min) was  $0.647 \pm 0.017$ , which is the maximum reaction rate constant of

each substance, and the minimum value of  $K_{\text{TN}}$  was  $0.258 \pm 0.083$ . If only the conversion of  $\text{NH}_4^+\text{-N}$  into  $\text{NO}_3^-\text{-N}$  under aerobic condition was considered, the converted  $K_{\text{NO}_3^-\text{-N}}$  will be about  $0.416 \pm 0.044$ , but the actual conversion to  $\text{NO}_3^-\text{-N}$  is not only the ammonification reaction of  $\text{NH}_4^+\text{-N}$ . The actual value of  $K_{\text{NO}_3^-\text{-N}}$  will be higher than 0.416. Ammonification reaction is the main way to convert  $\text{NH}_4^+\text{-N}$  to  $\text{NO}_3^-\text{-N}$ ; thus, other transformation ways are greatly affected by the reaction conditions. Here, we only calculated the  $\text{NH}_4^+\text{-N}$  ammonification reaction after weighted estimation. According to the size of the reaction rate constant, the reaction rates were in the order:  $K_{\text{COD}}$  ( $0.647 \pm 0.017$ ) >  $K_{\text{NO}_3^-\text{-N}}$  ( $0.416 \pm 0.044$ ) >  $K_{\text{NH}_4^+\text{-N}}$  ( $0.275 \pm 0.014$ ) >  $K_{\text{TN}}$  ( $0.258 \pm 0.083$ ). Therefore, the combined application system is a wastewater treatment system with high nitrogen removal efficiency dominated by COD removal. The removal rates of various pollutants were in the order of:  $\text{COD} > \text{NO}_3^-\text{-N} > \text{NH}_4^+\text{-N} > \text{TN}$ .

### 3.5 Variation of membrane contamination in the combined sewage treatment system

Membrane contamination is inevitable during the operation of the combined system. The system stops the sewage treatment operation and starts the membrane cleaning operation when the

membrane pressure difference reaches 50 kPa. The membrane cleaning system adopts full automatic control. The membrane pressure difference of the original MBR system reached 50 kPa between 5 and 7 days, whereas that of the combined system reached 50 kPa between 7 and 10 days. This finding indicates that the combined system effectively mitigated the membrane contamination. Compared with the original MBR system, the sludge settling performance of the combined system was remarkably improved, and the settling performance of the combined system can reach the settling effect of the original system (30 min) in 5 min.

### 3.6 Energy saving and carbon emission reduction measurement of the combined sewage treatment system

The sewage treatment scale of the railway station is 3,000 t/day, including six lifting pumps with a total operating power of 9 kW and six MBR wastewater processors with a total operating power of 99 kW. This scale translates into a daily power consumption of 1,903.2 kWh. According to the TN removal rate, which increased by three times conversion, a total of 1268.8 kW h/day energy saving was achieved, and the annual electricity saving was 463,112 kWh. The amount of membrane-cleaning water was 159.6 t/time, and the drug dosage was 1.92 t/day. The average membrane-cleaning volume was reduced from 61 times per year to 43 times, with a reduction of 18 times, saving 2,872.8 t of water and 34.54 t of drug consumption. According to CO<sub>2</sub> conversion, the annual reduction in electricity was 463,112 kWh, which corresponds to the carbon emission reduction of 363,542.92 kg CO<sub>2</sub>e; the water saved was 2,872.8 t, which corresponds to the carbon emission reduction of 482.63 kg CO<sub>2</sub>e; and the reduction in pharmaceutical dosage was 34.54 t, which corresponds to the comprehensive carbon emission reduction of 24,178 kg CO<sub>2</sub>e. Therefore, the annual carbon reduction of the combined system is at least 388,203.55 kg CO<sub>2</sub>e.

## 4 Conclusion

The results showed that ICMS-AS + MBR has a strong ability to resist the impacts of COD, NH<sub>4</sub><sup>+</sup>-N, and TP hydraulic loads. The COD, NH<sub>4</sub><sup>+</sup>-N, and TP values of raw water vary irregularly at 112.0–328.0, 16.0–42.0, and 2.0–6.0 mg/L, respectively, whereas the COD, TN, and TP values of the combined system were all stable in the ranges of 19.2–43.3, 2.1–3.4, and 0.3–0.4 mg/L, respectively. This finding indicates that the combined system has good resistance to hydraulic load impact and has stable effluent quality. Compared with the original MBR system without ICMC-AS, the COD, TN, and TP removal

efficiencies of the combined system increased from 80%, 30%, and 10% to 92%, 93.5%, and 92%, respectively.

The study of the operation efficiency and parameters of the combined system and the in-depth analysis of the reaction process and reaction rate of the iron–carbon microelectrolysis wastewater treatment system revealed that the combined system is a wastewater treatment system dominated by COD removal with high nitrogen removal efficiency. The removal rate constants of various pollutants were in the order:  $K_{\text{COD}} (0.647 \pm 0.017) > K_{\text{NO}_3\text{-N}} (0.416 \pm 0.044) > K_{\text{NH}_4\text{-N}} (0.275 \pm 0.014) > K_{\text{TN}} (0.258 \pm 0.083)$ .

Compared with the original MBR system, the combined system had a considerably improved sludge settling performance and can reach the settling effect of the original system (30 min) in 5 min. This performance effectively mitigated membrane contamination in the combined system.

The above results indicate that adding iron–carbon microelectrolysis activated sludge to the MBR processor for combined wastewater treatment can enhance the efficiency of wastewater treatment and obtain better energy-saving and emission-reducing effects. This combined application provides an effective way for the transformation and upgrading of small- and medium-scale water treatment systems.

## Data availability statement

The original contributions presented in the study are included in the article/supplementary material, further inquiries can be directed to the corresponding authors.

## Author contributions

All authors listed have made a substantial, direct, and intellectual contribution to the work and approved it for publication.

## Funding

This work was funded by the Science and Technology Research Project of the Education Department of Jiangxi Province, China (No. GJJ200632).

## Conflict of interest

The authors declare that the research was conducted in the absence of any commercial or financial relationships that could be construed as a potential conflict of interest.

## Publisher's note

All claims expressed in this article are solely those of the authors and do not necessarily represent those of their affiliated

organizations, or those of the publisher, the editors and the reviewers. Any product that may be evaluated in this article, or claim that may be made by its manufacturer, is not guaranteed or endorsed by the publisher.

## References

- Adav, S. S., and Lee, D.-J. (2011). Characterization of extracellular polymeric substances (EPS) from phenol degrading aerobic granules. *J. Taiwan Inst. Chem. Eng.* 42 (4), 645–651. doi:10.1016/j.jtice.2010.11.012
- Deng, S., Li, D., Yang, X., Xing, W., Li, J., and Zhang, Q. (2016a). Biological denitrification process based on the Fe(0)-carbon micro-electrolysis for simultaneous ammonia and nitrate removal from low organic carbon water under a microaerobic condition. *Bioresour. Technol.* 219, 677–686. doi:10.1016/j.biortech.2016.08.014
- Deng, S., Li, D., Yang, X., Zhu, S., and Li, J. (2016b). Process of nitrogen transformation and microbial community structure in the Fe(0)-carbon-based bio-carrier filled in biological aerated filter. *Environ. Sci. Pollut. Res.* 23 (7), 6621–6630. doi:10.1007/s11356-015-5892-6
- Deng, S., Peng, S., Xie, B., Yang, X., Sun, S., Yao, H., et al. (2020a). Influence characteristics and mechanism of organic carbon on denitrification, N<sub>2</sub>O emission and NO<sub>2</sub> – accumulation in the iron [Fe(0)]-oxidizing supported autotrophic denitrification process. *Chem. Eng. J.* 393, 124736. doi:10.1016/j.cej.2020.124736
- Deng, S., Xie, B., Kong, Q., Peng, S., Wang, H., Hu, Z., et al. (2020b). An oxic/anoxic-integrated and Fe/C micro-electrolysis-mediated vertical constructed wetland for decentralized low-carbon greywater treatment. *Bioresour. Technol.* 315, 123802. doi:10.1016/j.biortech.2020.123802
- Hu, Z., Deng, S., Li, D., Guan, D., Xie, B., Zhang, C., et al. (2020). Application of iron [Fe(0)]-rich substrate as a novel capping material for efficient simultaneous remediation of contaminated sediments and the overlying water body. *Sci. Total Environ.* 748, 141596. doi:10.1016/j.scitotenv.2020.141596
- Jiaohui, X., Dan, C., Cheng, H., Yan, L., Xinbai, J., and Jinyou, S. (2021). Reductive potential from cathode electrode as an option for the achievement of short-cut nitrification in bioelectrochemical systems. *Bioresour. Technol.* 338, 125553. doi:10.1016/j.biortech.2021.125553
- Meng, J., Li, J., Li, J., Antwi, P., Deng, K., Nan, J., et al. (2018). Enhanced nitrogen removal from piggery wastewater with high NH<sub>4</sub><sup>+</sup> and low COD/TN ratio in a novel upflow microaerobic biofilm reactor. *Bioresour. Technol.* 249, 935–942. doi:10.1016/j.biortech.2017.10.108
- Pellicer-Nacher, C., Domingo-Felez, C., Mutlu, A. G., and Smets, B. F. (2013). Critical assessment of extracellular polymeric substances extraction methods from mixed culture biomass. *Water Res. A J. Int. water Assoc.* 47 (15), 5564–5574. doi:10.1016/j.watres.2013.06.026
- Qi, Y., Wu, S., Xi, F., He, S., Fan, C., Dai, B., et al. (2016). Performance of a coupled micro-electrolysis, anaerobic and aerobic system for oxytetracycline (OTC) production wastewater treatment. *J. Chem. Technol. Biotechnol.* 91 (5), 1290–1298. doi:10.1002/jctb.4719
- Tong, W., Jie, D., Shan-Shan, Y., Le, Z., Bing-Feng, L., Guo-Jun, X., et al. (2022a). A novel cross-flow honeycomb bionic carrier promotes simultaneous nitrification, denitrification and phosphorus removal in IFAS system: Performance, mechanism and keystone species. *Water Res.* 225, 119132. doi:10.1016/j.watres.2022.119132
- Tong, W., Yang, S. S., Zhong, L., Pang, J. W., Zhang, L., Xia, X. F., et al. (2022b). Simultaneous nitrification, denitrification and phosphorus removal: What have we done so far and how do we need to do in the future? *Sci. total Environ.* 856, 158977. doi:10.1016/j.scitotenv.2022.158977
- Vleeschauwer, F. D., Caluwé, M., Dobbeleers, T., Stes, H., Dockx, L., Kiekens, F., et al. (2020). A dynamic control system for aerobic granular sludge reactors treating high COD/P wastewater, using pH and DO sensors. *J. Water Process Eng.* 33, 101065. doi:10.1016/j.jwpe.2019.101065
- Wang, W. Q., Li, D., Gao, X., and Zhang, J. (2021). Combining different aerobic/anoxic durations with zoned sludge discharge to optimize short-cut nitrification denitrifying phosphorus removal granules in domestic sewage. *Huan jing ke xue = Huanjing kexue* 42 (9), 4406–4413. doi:10.13227/j.hjkk.202102182
- Wu, S., Qi, Y., Fan, C., Dai, B., Huang, J., Zhou, W., et al. (2016). Improvement of anaerobic biological treatment effect by catalytic micro-electrolysis for monensin production wastewater. *Chem. Eng. J.* 296, 260–267. doi:10.1016/j.cej.2016.03.140
- Xing, W., Li, D., Li, J., Hu, Q., and Deng, S. (2016). Nitrate removal and microbial analysis by combined micro-electrolysis and autotrophic denitrification. *Bioresour. Technol.* 211, 240–247. doi:10.1016/j.biortech.2016.03.044
- Yadu, A., Sahariah, B. P., and Anandkumar, J. (2019). Novel bioremediation approach for treatment of naphthalene, ammonia-N and sulphate in fed-batch reactor. *J. Environ. Chem. Eng.* 7 (5), 103388. doi:10.1016/j.jece.2019.103388